ORIGINAL PAPER

Celso Sant'Anna · Loraine Campanati
Catarina Gadelha · Daniela Lourenço
Letícia Labati-Terra · Joana Bittencourt-Silvestre
Marlene Benchimol · Narcisa Leal Cunha-e-Silva
Wanderley De Souza

Improvement on the visualization of cytoskeletal structures of protozoan parasites using high-resolution field emission scanning electron microscopy (FESEM)

Abstract The association of high resolution field emission scanning electron microscopy (FESEM), with a more efficient system of secondary electron (SE) collection and in-lens specimen position, provided a great improvement in the specimen's topographical contrast and in the generation of high-resolution images. In addition, images obtained with the use of the high-resolution backscattered electrons (BSE) detector provided a powerful tool for immunocytochemical analysis of biological material. In this work, we show the contribution of the FESEM to the detailed description of cytoskeletal structures of the protozoan parasites *Herpetomonas megaseliae, Trypanosoma brucei* and *Giardia lamblia*. High-resolution images of detergent extracted *H. megaseliae* and *T. brucei* showed the profile of the cortical microtubules, also known as sub-pellicular microtubules (SPMT), and protein bridges cross-linking them. Also, it was possible to visualize fine details of the filaments that form the lattice-like structure of the paraflagellar rod (PFR) and its connection with the axoneme. In *G. lamblia*, it was possible to observe the intricate structure of the adhesive disk, funis (a microtubular array) and other cytoskeletal structures poorly described previously. Since most of the stable cytoskeletal structures of this protozoan rely on tubulin, we used the BSE images to accurately map immunolabeled tubulin in its cytoskeleton. Our results suggest that the observation of detergent extracted parasites using FESEM associated to backscattered analysis of immunolabeled specimens represents a new approach for the study of parasite cytoskeletal elements and their protein associations.

Keywords Protozoa · Cytoskeleton · Field emission scanning electron microscopy · Immunolabeling · Trypanosomatids · *Giardia lamblia*

C. Sant'Anna · L. Campanati · C. Gadelha · D. Lourenço
L. Labati-Terra · J. Bittencourt-Silvestre
N. L. Cunha-e-Silva · W. De Souza (✉)
Laboratório de Ultraestrutura Celular Hertha Meyer,
Instituto de Biofísica Carlos Chagas Filho,
Universidade Federal do Rio de Janeiro CCS, Rio de Janeiro,
bloco G, Cidade Universitária, 21949-900, Brazil
E-mail: wsouza@biof.ufrj.br
Tel.: +55-21-25626583
Fax: +55-21-22602364

M. Benchimol
Laboratório de Ultraestrutura Celular,
Universidade Santa Úrsula, R. Jornalista Orlando Dantas,
59, Rio de Janeiro, Brazil

Introduction

In the scanning electron microscope (SEM), a thin and focused spot of electrons scans the surface of an electrically conductive specimen. Resolution in SEM is limited mainly by the probe size and the interaction volume between the primary electron probe and the sample (Joy and Pawley 1992). Due to limitations in electron optical design, resolution in conventional scanning electron microscope (CSEM) is limited to 15–20 nm, therefore making it impossible to resolve thin details of the sample. A considerable improvement on scanning electron microscopy images was the introduction of stable cold field emission scanning electron microscope (FESEM). FESEM produces images whose resolution is comparable with transmission electron microscope (TEM) (Apkarian 1997; Pawley 1997). In addition, advantage in ultra-thin metal film coating techniques associated with the higher resolution has allowed improvements concerning the acquisition of topographic details and contrast using the FESEM (Peters 1979).

Gold markers have been extensively used in immunocytochemistry analysis in SEM. Backscattered elec-

tron (BSE) images, which are based on atomic number contrast, permitted discernible visualization of the gold marker and analysis of the sample surface. The resolution power of the FESEM coupled with high-sensitive yttrium aluminum garnet (YAG) BSE detector achieved unambiguous gold marker localization and the visualization of gold particles of about 1 nm as well as the achievement of higher topographic contrast (reviewed by Hermann et al. 1996).

Protozoan parasites are the causative agents of several important social-economic diseases spread over the world, such as *Leishmania spp.*, *Trypanosoma brucei*, *Trypanosoma cruzi*, *Entamoeba histolytica*, *Giardia lamblia*, among others. These protozoa are the subjects of many studies since they possess characteristic structures that are not found in most of the eukaryotic cells. One of these is their unusual cytoskeleton. As well described by light and TEM, it has an arrangement that contrasts with mammalian cell cytoskeleton and, in the case of *Giardia*, it is thought that the cytoskeleton itself works as a virulence factor (Elmendorf et al. 2003).

The cytoskeleton of trypanosomatids is complex and stable, composed of interesting systems, namely, the sub-pellicular microtubules (SPMT), the flagellum axoneme and its adjacent paraflagellar rod (PFR), a flagellum attachment zone (FAZ) and cytostome-associated microtubules (De Souza 1988; Gull 1999). The SPMT form a layer of regularly spaced singlet microtubules, underlying the plasma membrane, along the cell body. They confer an unusual resistance to mechanical lysis and contribute to the stabilization of the protozoan shape. In contrast to the microtubules of mammalian cells, SPMT are resistant to low temperature and colchicine treatment (MacRae and Gull 1990) that usually promotes microtubule depolymerization. Drugs that could disrupt these microtubules are rare, and would constitute potential chemotherapeutic agents.

The PFR is a cytoskeletal structure formed by filaments assembled in a complex way (Farina et al. 1986). It runs along with the axoneme (AX), being connected to the outer doublets 4–7 (Fuge 1969; De Souza and Souto-Padrón 1980). PFR function is not completely understood, although it is undoubtedly essential to flagellar movement (Bastin et al. 1998).

The trophozoite form of *G. lamblia* has a complex stable cytoskeleton (built mainly by microtubular systems) that helps its attachment to the epithelial cells of the small intestine of vertebrates and also in the parasite displacement (Adam 2001; Campanati et al. 2002, 2003; Elmendorf et al. 2003). The *Giardia* trophozoite presents eight flagella arranged in four pairs, each one contributing differently to the global movement (Ghosh et al. 2001; Campanati et al. 2002; Elmendorf et al. 2003). Beside that, it exhibits in its most anterior region the adhesive disk (AD), an intricate structure made up of spirally arranged microtubules, micro-ribbons and cross bridges that has often been referred to as responsible for the cell attachment (Holberton 1973; Adam 2001; Ghosh et al. 2001; Campanati et al. 2002; Elmendorf

et al. 2003). The basal bodies of the eight flagella lie deeply in the cell body; this is also the origin of the funis, a microtubular array that follows the axonemes of the caudal flagella and is also involved in the cell movement (Campanati et al. 2002; Campanati et al. 2003; Benchimol et al. 2004). Small bridges, whose composition has not yet been clarified, connect funis microtubules. The median body, another cytoskeletal structure of *Giardia* is also formed by an array of microtubules, this time organized transversally to the cell axis. Its function is not known, although some hypotheses have been proposed (Crossley et al. 1986; Marshal and Holberton 1993; Campanati et al. 2003; Elmendorf et al. 2003).

In this paper, we report a new protocol to study the cytoskeleton of protozoan parasites using membrane detergent extraction and high-resolution FESEM. Using this strategy, fine details of parasite cytoskeletal elements, such as SPMT, axonemes, PFR and flagella connector (FC) in trypanosomatids and adhesive disk, median body and funis in *G. lamblia* were clearly observed.

Materials and methods

Parasites

Herpetomonas megaseliae promastigotes were axenically cultivated in liver infusion tryptose (LIT) medium (Camargo 1964) supplemented with 5% fetal calf serum (FCS), at 28°C. Procyclic trypomastigotes of *T. brucei* strain 457 were cultivated in SDM-79 (Brun and Schönenberger 1979) supplemented with 10% fetal calf serum. *Giardia lamblia* trophozites (WB strain) were cultivated in TYI-S-33 medium supplemented with 10% bovine adult serum, 0.1% bovine bile (Keister 1983) at 37°C.

Field emission scanning electron microscopy

Parasites were washed twice in phosphate buffered saline solution (PBS: 0.02 M Na_2HPO_4, 0.02 M NaH_2PO_4, 0.9% NaCl, pH 7.2) and allowed to adhere in 0.1% poly-L-lysine-coated glass coverslips for 10 min in the case of the trypanosomatids and 2 min for *Giardia* trophozoites, at room temperature. The protozoa were extracted with 1% Nonidet P-40 in 0.1 M PHEM buffer [60 mM 1,4 piperazine diethylsulfonic acid (PIPES), 25 mM N-2-hydroxyethylpiperazine Nl-2-ethanesulfonic acid (HEPES), 10 mM EGTA, and 2 mM $MgCl_2$ (Schliwa and van Blerkom 1981)] pH 7.2 for 10 min at room temperature, washed in 0.1 M PHEM and fixed with 2.5% glutaraldehyde in 0.1 M PHEM buffer for 20 min, washed again in 0.1 M PHEM, dehydrated in ethanol series (50, 70, 90 and 100%), critical point-dried in a Baltec CPD 030 apparatus and mounted on specimen stubs. The samples were ion-sputtered to avoid charge effect with 2–3 nm carbon layer using a Gatan

681 high-resolution ion beam coat at an angle of 45°. Argon ion beam sputter was operated at 6 mA at an acceleration voltage of 10 kV. Secondary electron (SE) images were obtained in JEOL JSM-6340 FESEM at accelerating voltage of 5.0 kV at 12 μA emission current and work distance at 8 mm.

Immunocytochemistry

Parasites were extracted as described above and fixed with 4% paraformaldehyde in 0.1 M PHEM buffer for 30 min. The sample were washed and incubated with 50 mM ammonium chloride in 0.1 M PHEM buffer for 15 min in order to quench free aldehyde groups. The cells were further incubated in PBS containing 1.5% bovine albumin, 0.5% fish gelatine and 0.02% Tween 20, pH 8.0 (blocking buffer) for 1 h at room temperature. The incubation with the primary antibody (anti-α-tubulin, TAT-1, generously provided by Dr. Keith Gull and # 5168 clone B-512 anti-α-tubulin from Sigma) was performed for 1 h at room temperature. After washing with blocking buffer, the samples were incubated with the secondary antibody, goat anti-mouse IgG-15 nm gold (BBInternational, 1:100) for 1 h at room temperature. Controls were achieved by replacing the primary antibodies for blocking buffer. After incubation, the samples were fixed in 2.5% glutaraldehyde in 0.1 M PHEM, dehydrated and treated as described above. For immunogold labeling observation, the samples were coated with a thin carbon film using Gatan 681 high-resolution ion beam coat at an angle of 45°. Argon ion beam sputter was operated at 6 mA at an acceleration voltage of 10 kV. BSE images were obtained in JEOL JSM-6340 FESEM coupled with a cerium doped YAG backscattered detector. The FESEM was operated in BSE mode to image cytoskeleton elements labeled with gold particles. Alternatively, the microscope was operated in LEI mode, which produces images generated by both SE and BSE detectors. In both modes, the accelerating voltage was 5.0 kV at 12 μA emission current, work distance 8 mm and the largest condenser aperture (120 μm) to optimal BSE collection.

Results

Ultrastructural analysis of H. megaseliae and T. brucei cytoskeleton by high-resolution FESEM

In high-resolution (SE) images of detergent extracted H. megaseliae and T. brucei, we could clearly resolve the individual microtubules that form the sub-pellicular microtubule (the SPMT) array that runs parallel along the whole cell body (Fig. 1a–d), except for the flagellar pocket (Fig. 1f). Microtubules in H. megaseliae are helically disposed (Fig. 1a), whereas in T. brucei they present a straight pattern (Fig. 1b). Higher magnification shows the precise organization of short filaments that connect the microtubules to each other (Fig. 1c, arrows). Examination of parasite flagellar structures allowed clear observation of the PFR that runs alongside the microtubule doublets that form the axoneme (AX) as well as its association with the PFR (Fig. 1e). Topographic contrast at high magnification in FESEM image of PFR distal domain provided ready visualization of its filamentous features. They are periodically arranged as large and thin individual crossing filaments (Fig. 1g). In dividing T. brucei, the flagella connector (FC) can be easily recognized, localized on the tip of the new flagellum (NF) and is laterally attached to the axoneme of the old one (Fig. 1b, h).

High-resolution FESEM images of G. lamblia

FESEM images show that the adhesive disk microtubular spiral array begins somewhere close to the basal bodies of the flagella. The detergent extraction exposed an area known as the "bare area", where the basal bodies are found, as well as the possible origin of the AD (Fig. 2a, d, e). Structures associated to the basal bodies, known as the banded collars (BC1/BC2), firstly described by Crossley et al. (1986), were clearly recognizable (Fig. 2a, d, e). The microtubules of the AD and the cross-bridges were easily distinguished (Fig. 2a). In the funis, most of these microtubules are parallel to the axoneme of the caudal flagella and, by this method, we were able to observe how they are distributed along the posterior region of the cell, how they interact with the axoneme of the caudal and posterior pairs of flagella and thus contribute to the parasite movement, as the lateral flexion of the tail (Fig. 2b,c; Benchimol et al. 2004). High-resolution FESEM images of single microtubules allowed us to make functional propositions starting from structural observations. Besides the structures described above, we could observe structures associated with the axoneme of the anterior flagella, namely the dense rods and marginal plates (Fig. 2f, g). The latter were also previously described by routine TEM, but their analysis by negative staining was not made, since it was supposed that they were sensitive to detergent treatment (Friend 1966; Holberton 1973).

Immuno-FESEM

In a previous paper from our group (Campanati et al. 2003), we studied tubulin diversity in trophozoites of Giardia by the use of several antibodies. In the present paper, we used two of those antibodies, this time taking the advantage of high-resolution BSE detector coupled to the FESEM. In addition, we associated membrane extraction to colloidal gold labeling. FESEM images allowed us to visualize even single microtubules labeled with both antibodies used in this study. The antibody #5168 showed intense staining in the caudal, lateral and ventral flagella (Fig. 3a–c). A light colloidal gold decoration was

Fig. 1 FESEM images of whole
extracted *H. megaseliae* (**a, c, e,
g**) and *T. brucei* (**b, d, f, h**) show
SPTM parallel to each other,
except for the flagellar pocket
(FP—f). **a** Helical pattern of *H.
megaseliae* cytoskeleton.
Figure 2b, d the straight pattern
found in *T. brucei* cytoskeleton.
In higher magnification, it was
clearly possible to resolve the
bridges (*arrows*) that connect
microtubules to each other. **e** It
is observed that the
paraflagellar rod (*PFR*) runs
alongside the axoneme (Ax).
g It is possible to readily
visualize the large (*arrows*) and
thin (*arrowheads*) crossing
filaments in the distal domain of
PRF. **b, h** Show the flagella
connector (*arrow*) localized in
the tip of new flagellum (NF),
which is laterally attached to
AX of the old flagellum (OF) in
the dividing *T. brucei*. *Bars*:
a 3.5 µm, **b** 8 µm, **c** 1 µm,
d 2.6 µm, **e** 2.6 µm, **f** 1.6 µm,
g 0.5 µm, **h** 1.8 µm
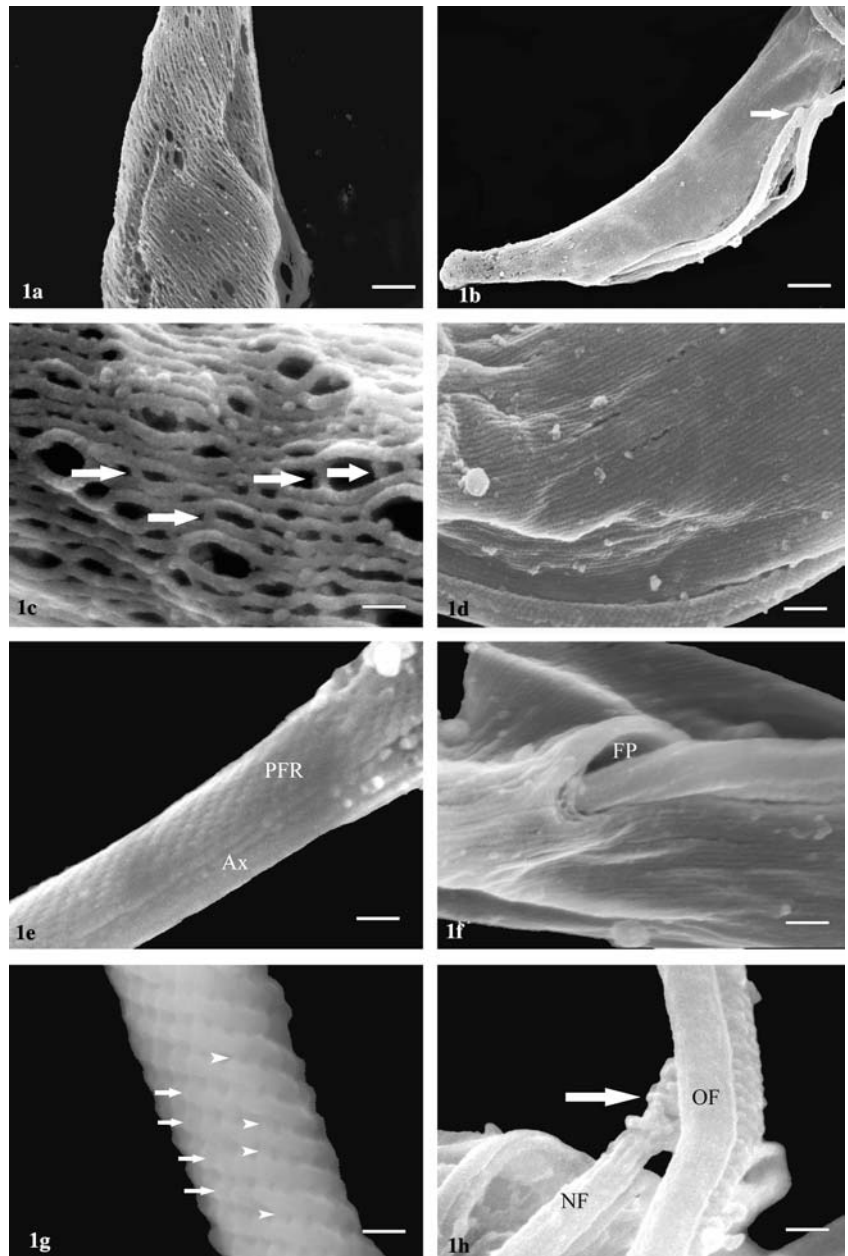
observed in other cytoskeleton elements, whereas using
the antibody TAT-1 the gold marker was observed in the
flagella, adhesive disk, funis and highly concentrated in
the median body (Fig. 3d–f). In backscattered images it
was possible to clearly distinguish the gold marker, al-
though cytoplasmic elements were not so evidently ob-
served (Fig. 3). Therefore, to improve the visualization of
cytoskeleton elements and colloidal gold labeling, we used
the LEI mode device, which is a combined collection of SE
and BSE electrons. It was possible to achieve better
information of gold marker localization in *Giardia* cyto-
skeleton elements (Fig. 3c, f). Using FESEM, we con-
firmed the previous results obtained by
immunofluorescence microscopy and established the
precise association between filaments and gold marker.

Discussion

Several electron microscopy techniques have been used
to study the cytoskeleton structures of protozoan para-
sites, each one with its own limitations. In routine TEM,
images of parasites and their cytoskeleton components
are obtained, in which they appear randomly orientated
in ultra-thin sections. Thus, it is not possible to determine
the exact three-dimensional distribution of such struc-
tures, unless one uses the 3D-reconstruction technique.
In negative staining, the samples are submitted to air-
drying. During this procedure, the surface tension in the
air/water interface causes the shrinkage and flattening of
the sample. Freeze etching has produced excellent images

◄
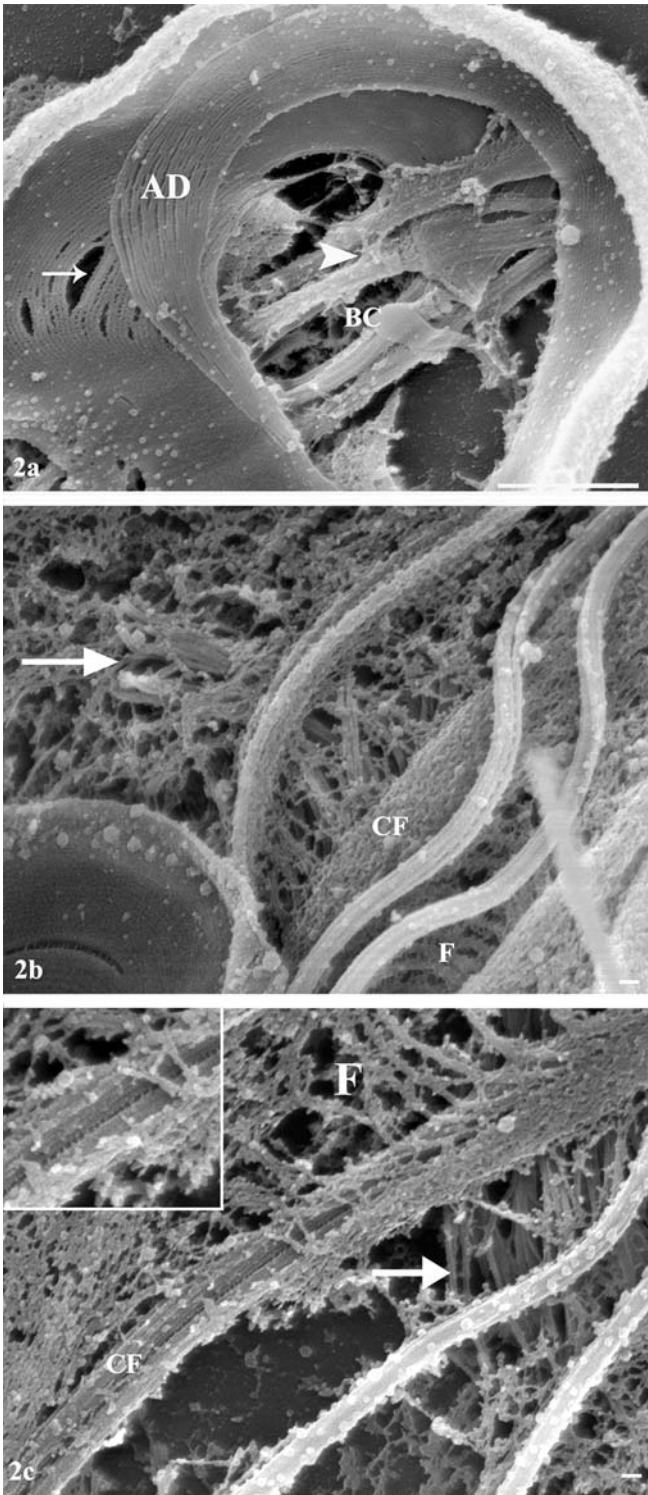
Fig. 2 *Giardia lamblia's* cytoskeleton as observed in FESEM. **a, b, c** General aspect of the cell after membrane extraction and prepared as described in material and methods for FESEM visualization. **a** The bare area of the adhesive disk (AD) is depicted and one can observe the point where the flagella (*arrowhead*) begin and one banded collar (BC). Besides, the bridges connecting the AD microtubules are also seen (*arrow*). **b, c** Microtubules of the median body (*arrows*) and funis (*F*), respectively. The caudal flagella (*CF*) AX are involved by a material of fibrillar nature and connected by slender bridges of an unknown nature (*inset*). **d** Low-magnification view of the extracted cell. The bare zone (*BZ*—central area of the AD) is clearly recognizable and also elements knows as banded collars (*BC1/BC2*). **e** Structures are shown in detail. It is believed that they are involved in microtubule nucleation. **f** Most anterior region of two cells. In the cell on the left side, it is possible to observe the lateral flange (*LF*) and its marginal plates (*MP*). The dense rod (*DR*) of one of the two anterior flagellae (*AF*) is also shown. In higher magnification (**g**), the structure of the marginal plate (*MP*) can be better analyzed, as well as the dense rod (*DR*) associated to one AF. *Bars*: **a**, **d** 1 μm, **b**, **e**, **f**, **g** 100 nm and **c** 100 nm

being frozen, the sample is randomly fractured and the region of interest may not be exposed. Finally, the sample is slightly heated to promote deep etching and rotatory shadowing. Therefore, the success in this technique is relatively low. One promising technique to overcome these problems is the improvement of the preparative methods followed by imaging in high-resolution FE-SEM. In this paper, we suggest the FESEM as an improved method for the study of protozoan cytoskeleton. The cold field emission gun combined with short focal-length lens has increased electron optical performance. New developments concerning electron optical design led FESEM to be comparable with TEM and overcome (CSEM) in terms of resolution and topographic contrast (reviewed by Pawley 1997). In addition, FESEM images equal macromolecular information produced by quick-freeze and platinum-carbon replica in TEM and section preparation (Apkarian 1997).

Mammalian cell cytoskeleton is a highly complex fibrillar system composed of actin microfilaments, intermediate filaments and microtubules. They are responsible for establishing cell shape, motility, division and intracellular transport. In addition, the labile mammalian cytoskeleton is largely regulated by the environment (reviewed by Heidemann and Wirtz 2004). In contrast, stable protozoan cytoskeleton is composed predominantly by microtubules and one can observe particular arrangements that are different from cell to cell. Neither intermediate filaments nor actin microfilaments have been visualized in the protozoa used in this study, although short actin filaments have recently been detected by immunofluorescence and immunocytochemistry in *Leishmania donovani* (Sahasrabuddhe et al. 2004) and bloodstream forms of *T. brucei* (Garcia-Salcedo et al. 2004).

In order to examine parasite cytoskeletal structures as a whole, we have slightly modified the most used protocols for cytoskeleton visualization. Our procedure is based on parasite extraction, fixation, dehydration,

of parasite cytoskeleton (Souto-Padrón et al. 1984; Kattenbach et al. 1996). However, it has many critical steps: the sample is quickly frozen to avoid crystal ice formation during the freezing and sublimation steps, and in many cases structure displacements are observed. In addition, it is difficult to obtain the adequate layer of water above the material, which must be thin enough to get the crystal ice formation for entire sample. After
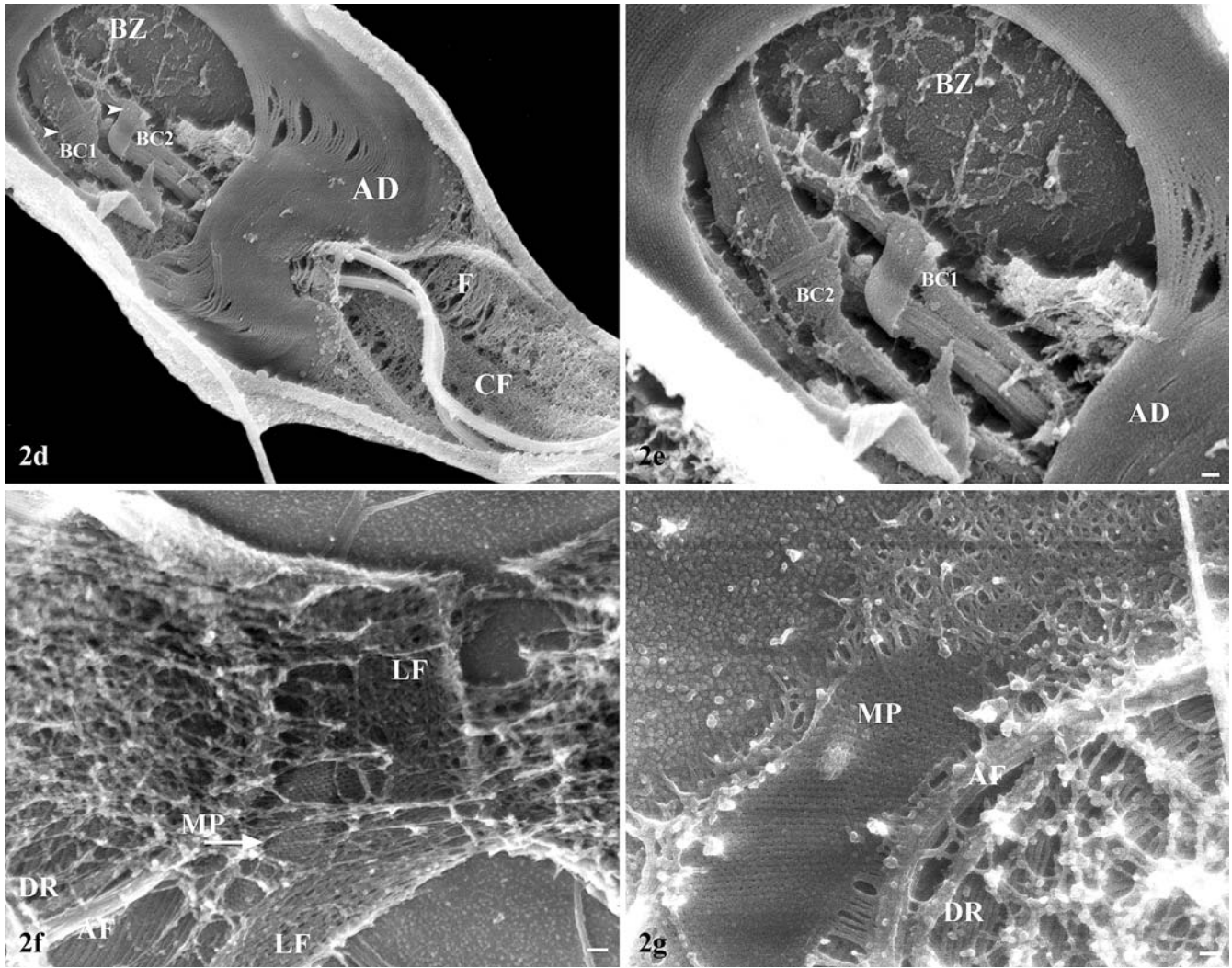
Fig. 2 (Contd.)

critical point drying, ultra-thin coating and finally takes advantage of the FESEM high-resolution power. This microscope yielded global high resolution images of the detergent extracted *H. megaseliae, T. brucei* and *G. lamblia*.

Parasites of the Trypanosomatidae family have an interesting cytoskeleton composed of a set of parallel stable SPMT. They are connected to each other and to the plasma membrane by short protein filaments. The SPMT play an important role in the maintenance of parasite shape. The precise organization of this structure varies significantly among the evolutive forms and during parasite differentiation (reviewed by De Souza 1988; Gull 1999). In this paper, we have taken advantage of topographic high-resolution images provided by FE-SEM, which allowed clear and faithful visualization of the whole protozoan cytoskeletal organization that is not possible to achieve using the techniques described earlier. In addition, it was possible to clearly resolve the filamentous structures that connect SPMT to each other

(Fig. 1c). TEM of thin sections of trypanosomatids have shown that the SPTM complex is composed of about 100 microtubule profiles underlying the parasite surface, with small variations among trypanosomatid species. Individual microtubules present a diameter of 25 nm regularly spaced at intervals of 18–22 nm forming a helical or straight pattern (Meyer and De Souza 1976; Gull 1999). Using the scalar mode device of the FESEM, similar thickness and distances between filaments were found (data not shown), in accordance with the results previously described. These observations indicate that thin carbon coating did not significantly alter the cytoskeleton filament thickness.

Trypanosomatids present an interesting lattice-like structure attached to the axoneme, named PFR (De Souza and Souto-Padrón 1980). This structure is formed by a complex array of 25 nm thick filaments crossed by others of 7 nm at an angle of 100° (Souto-Padrón et al. 1984; Farina et al. 1986). The organization of the various filaments, which form the PFR (Fig. 1e, g) and its attachment to axoneme (Fig. 1e) could be readily observed in FESEM high resolution images. In addition, FESEM images revealed the structure of the flagella
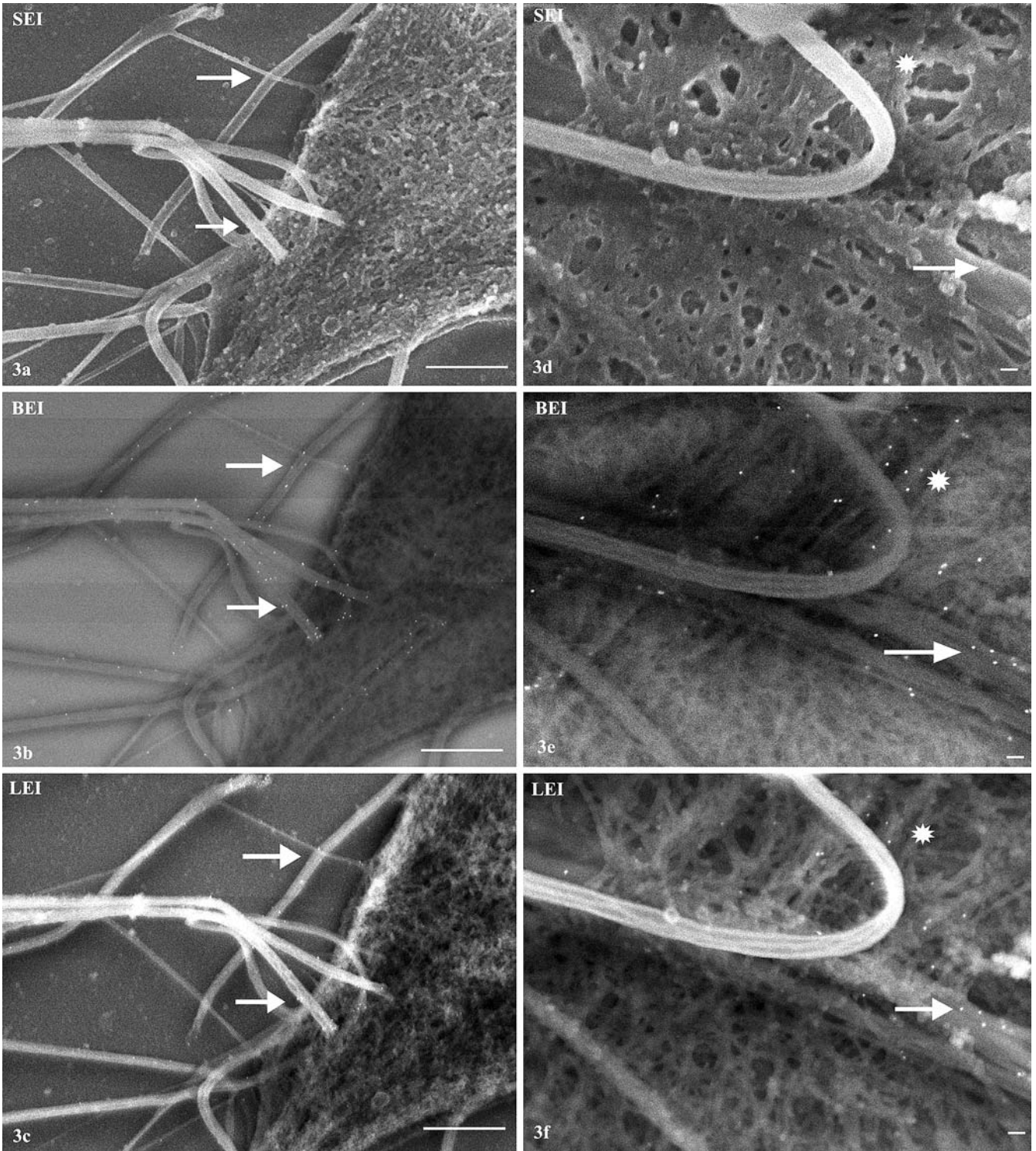
Fig. 3 Immunolabeling of cytoskeletal components. **a–f** Images obtained by the secondary electrons detector (*SEI*), backscattered electrons detector (*BEI*) and a mix of both detectors (*LEI*), respectively. **a–c** Immunolocalization of #5168 clone B-512 antibody to the flagella (*arrows*). **d–f** Localization of α-tubulin in the flagella (*arrows*) and median body (*asterisk*) using TAT-1 antibody. More details about the recognition pattern of these antibodies can be obtained in Campanati et al. 2003. *Bars*: **a–c** 1 μm and **d–f** 100 nm

connector that was firstly visualized by negative staining in dividing *T. brucei* (Moreira-Leite et al. 2001). The FC, a mobile transmembrane junction whose molecular nature is unknown, is observed at the distal tip of new flagella and it is connected to the old flagellar axoneme (Briggs et al. 2004). The FC structure was previously characterized as formed by three domains: a "fuzzy" region, a short-link structure and a lamellar plate com-

ponent connected to old flagellum (OF). In high-resolution FESEM images the FC structure was clearly discernible (Fig. 1h).

The cytoskeleton of *G. lamblia* has been the subject of several morphological studies (Friend 1966; Holberton 1973, 1981; Holberton and Ward 1981; Crossley and Holberton 1983; Elmendof et al. 2003). This protozoan is referred to as one of the most anciently branching eukaryotes, although sometimes it has been contradicted (Tovar et al. 2003). Nevertheless, taking into account the disease caused by the colonization of the small intestine by this parasite, it is of critical importance to determine the exact association of structure and function of each of *Giardia's* cytoskeletal structure, since, as suggested by Elmendorf in a recent review (Elmendorf et al. 2003), in this cell, there is apparently a strong link between the cytoskeleton and virulence.

Crossley and co-workers (1986) described four microtubular sets in *Giardia*: disk cytoskeleton (comprising the banded collars), axoneme of the eight flagella (that were not being described here), funis and median body. Detergent treatment to expose cytoskeleton elements from *Giardia* by negative staining technique was already used in previous reports (Holberton 1981; Holberton and Ward 1981; Crossley et al. 1986). As already described, this technique has several disadvantages, although it has been the responsible for the description of great part of the internal structure of *Giardia*.

As described by Erlandsen et al. (2003), the use of BSE imaging in field emission microscopes allows atomic number contrast achievement while simultaneously collecting topographical information. It means that, in this way, one can detect colloidal gold particles in metal sputtered specimens and, at the same time, acquire high-resolution images of the specimen. As also stated, the resolution depends on a number of factors, including metal coat thickness and the BSE detector used. In our experiments, these factors were optimized in order to achieve the best correlation between image formation and colloidal gold particle detection.

The development of the FESEM, which can achieve limits of resolution comparable to the TEM, has opened a new opportunity to the understanding of the internal structures of several cells, including *Giardia*. Using protocols similar to those used by others, it was possible to better observe the structural organization of the adhesive disk, funis, marginal plates, dense rods and median body, avoiding the problems related to thin sectioning or air drying.

Field emission scanning electron microscope in combination with high-resolution BSE detector provides useful gold labeled antigen localization (Erlandsen et al. 2003). In this work, using different antibodies raised against tubulin we confirmed the results obtained in previous reports on the tubulin diversity of *Giardia* trophozoites (Campanati et al. 2003) and on the structure and function of the funis (Benchimol et al. 2004).

In summary, we observed no difference in general morphology and in protozoan cytoskeleton arrangement from what have been previously described by routine TEM, negative staining and freeze etching techniques. However, in contrast to other methodologies often used for cytoskeleton visualization, combined detergent extraction and critical point drying coupled with FESEM analysis allowed us to expose preserved cytoskeletons, allowing the acquisition of high-quality topographic contrast images of protozoan cytoskeletal component organization as a whole. Beside that, using high-resolution BSE detector it was possible to precisely map its tubulin content. For that reason, we propose that high-resolution FESEM offers new perspectives on the study of protozoan parasite cytoskeleton structures.

References

Adam RD (2001) Biology of *Giardia lamblia*. Clin Microbiol Rev 14:447–475

Apkarian RP (1997) The fine structure of fenestrated adrenocortical capillaries revealed by in-lens field-emission scanning electron microscopy and scanning transmission electron microscopy. Scanning 19:361–367

Bastin P, Sherwin T, Gull K (1998) Paraflagellar rod is vital for trypanosome motility. Nature 391:548

Benchimol M, Piva B, Campanati L, De Souza W (2004) Visualization of the funis of *Giardia lamblia* by high-resolution field emission scanning electron microscopy—new insights. J Struct Biol 147:102–115

Briggs LJ, McKean PG, Baines A, Moreira-Leite F, Davidge J, Vaughan S, Gull K (2004) The flagella connector of *Trypanosoma brucei*: an unusual mobile transmembrane junction. J Cell Sci 117:1641–1651

Brun R, Schönenberger M (1979) Cultivation and in vitro cloning of procyclic culture forms of *Trypanosoma brucei* in a semi-defined media. Acta Trop 36:289–292

Camargo EP (1964) Growth and differentiation in *Trypanosoma cruzi*. I. Origin of metacyclic trypanosomes on liquid media. Rev Inst Med Trop São Paulo 12:93–100

Campanati L, Holloschi A, Troster H, Spring H, De Souza, Monteiro-Leal LH (2002) Video-microscopy observations of fast dynamic processes in the protozoon *Giardia lamblia*. Cell Motil Cytoskeleton 51:213–224

Campanati L, Troester H, Monteiro-Leal LH, Spring H, Trendelenburg MF, De Souza W (2003) Tubulin diversity in trophozoites of *Giardia lamblia*. Histochem Cell Biol 119:323–331

Crossley R, Holberton DV (1983) Characterization of proteins from the cytoskeleton of *Giardia lamblia*. J Cell Sci 59:81–103

Crossley R, Marshall J, Clark JT, Holberton DV (1986) Immunocytochemical differentiation of microtubules in the cytoskeleton of *Giardia lamblia* using monoclonal antibodies to alpha-tubulin and polyclonal antibodies to associated low molecular weight proteins. J Cell Sci 80:233–252

De Souza W (1988) The cytoskeleton of trypanosomatids. Mem Inst Oswaldo Cruz 83:546–560

De Souza W, Souto-Padrón T (1980) The paraxial structure of the flagellum of trypanosomatidae. J Parasitol 66(2):229–236

Elmendorf HG, Dawson SC, McCaffery JM (2003) The cytoskeleton of *Giardia lamblia*. Int J Parasitol 33:3–28

Erlandsen S, Chen Y, Frethem C, Detry J, Well C (2003) High-resolution backscatter electron imaging of colloidal gold in LVSEM. J Microsc 211:212–218

Farina M, Attias M, Souto-Pádron T, De Souza W (1986) Further studies on the structural organization of the paraxial structure of Trypanosomatids. J Protozool 33:552–557

Friend DS (1966) The fine structure of *Giardia muris*. J Cell Biol 29:317–332

Fuge H (1969) Electron microscopic studies of the intraflagellar structures of trypanosomes. J Protozool 16:160–166

Garcia-Salcedo JA, Perez-Morga D, Gijon P, Dilbeck V, Pays E, Nolan DP (2004) A differential role for actin during the life cycle of *Trypanosoma brucei*. EMBO J 23:780–789

Ghosh S, Frisardi M, Rogers R, Samuelson J (2001) How *Giardia* swim and divide. Infect Immun 69:7866–7872

Gull K (1999) The cytoskeleton of trypanosomatid parasites. Annu Rev Microbiol 53:629–655

Heidemann SR, Wirtz D (2004) Towards a regional approach to cell mechanics. Trends Cell Biol 14:160–166

Hermann R, Walther P, Muller M (1996) Immunogold labeling in scanning electron microscopy. Histochem Cell Biol 106:31–39

Holberton DV (1973) Fine structure of the ventral disk apparatus and the mechanism of attachment in the flagellate *Giardia muris*. J Cell Sci 13:11–41

Holberton DV (1981) Arrangement of subunits in microribbons from *Giardia*. J Cell Sci 47:167–185

Holberton DV, Ward AP (1981) Isolation of the cytoskeleton from *Giardia*. Tubulin and a low-molecular-weight protein associated with microribbon structures. J Cell Sci 47:139–166

Joy DC, Pawley JB (1992) High-resolution scanning electron microscopy. Ultramicroscopy 47:80–100

Kattenbach WM, Diniz Junior JA, Benchimol M, De Souza W (1996) A deep-etch study of the cytoskeleton of *Giardia duodenalis*. Biol Cell 86:161–166

Keister DB (1983) Axenic culture of *Giardia lamblia* in TYI-S-33 medium supplemented with bile. Trans R Soc Trop Med Hyg 77:487–488

MacRae TH, Gull K (1990) Purification and assembly in vitro of tubulin from *Trypanosoma brucei brucei*. Biochem J 265:87–93

Marshall J, Holberton DV (1993) Sequence and structure of a new coiled coil protein from a microtubule bundle in *Giardia*. J Mol Biol 231:521–530

Meyer H, De Souza W (1976) Electron microscopic study of *Trypanosoma cruzi* periplast in tissue cultures. I. Number and arrangement of the peripheral microtubules in the various forms of the parasite's life cycle. J Protozool 23:385–390

Moreira-Leite FF, Sherwin T, Kohl L, Gull K (2001) A trypanosome structure involved in transmitting cytoplasmic information during cell division. Science 294:610–612

Pawley J (1997) The development of field-emission scanning electron microscopy for imaging biological surfaces. Scanning 19:324–336

Peters KR (1979) Scanning electron microscopy at macromolecular resolution in low energy mode on biological specimens coated with ultra thin metal films. Scan Electron Microsc 2:133–148

Sahasrabuddhe AA, Bajpai VK, Gupta CM (2004) A novel form of actin in *Leishmania*: molecular characterisation, subcellular localisation and association with subpellicular microtubules. Mol Biochem Parasitol 134:105–114

Schliwa M, van Blerkom J (1981) Structural interaction of cytoskeletal components. J Cell Biol 90:222–235

Souto-Padrón T, De Souza W, Heuser JE (1984) Quick-freeze, deep-etch rotary replication of *Trypanosoma cruzi* and *Herpetomonas megaseliae*. J Cell Sci 69:167–178

Tovar J, Leon-Avila G, Sanchez LB, Sutak R, Tachezy J, van der Giezen M, Hernandez M, Muller M, Lucocq JM (2003) Mitochondrial remnant organelles of *Giardia* function in iron-sulphur protein maturation. Nature 426:172–176